



Fermi National Accelerator Laboratory

FERMILAB-Pub-97/024-E

CDF

J/ψ and $\psi(2S)$ Production in $p\bar{p}$ Collisions at $\sqrt{s} = 1.8$ TeV

F. Abe et al.

The CDF Collaboration

*Fermi National Accelerator Laboratory
P.O. Box 500, Batavia, Illinois 60510*

February 1997

Submitted to *Physical Review Letters*

Disclaimer

This report was prepared as an account of work sponsored by an agency of the United States Government. Neither the United States Government nor any agency thereof, nor any of their employees, makes any warranty, expressed or implied, or assumes any legal liability or responsibility for the accuracy, completeness, or usefulness of any information, apparatus, product, or process disclosed, or represents that its use would not infringe privately owned rights. Reference herein to any specific commercial product, process, or service by trade name, trademark, manufacturer, or otherwise, does not necessarily constitute or imply its endorsement, recommendation, or favoring by the United States Government or any agency thereof. The views and opinions of authors expressed herein do not necessarily state or reflect those of the United States Government or any agency thereof.

Distribution

Approved for public release; further dissemination unlimited.

J/ψ and $\psi(2S)$ Production in $p\bar{p}$ Collisions at $\sqrt{s} = 1.8$ TeV.

F. Abe,¹⁶ H. Akimoto,³⁵ A. Akopian,³⁰ M. G. Albrow,⁷ S. R. Amendolia,²⁶ D. Amidei,¹⁹
 J. Antos,³² S. Aota,³⁵ G. Apollinari,³⁰ T. Asakawa,³⁵ W. Ashmanskas,¹⁷ M. Atac,⁷ F. Azfar,²⁵
 P. Azzi-Bacchetta,²⁴ N. Bacchetta,²⁴ W. Badgett,¹⁹ S. Bagdasarov,³⁰ M. W. Bailey,²¹
 J. Bao,³⁸ P. de Barbaro,²⁹ A. Barbaro-Galtieri,¹⁷ V. E. Barnes,²⁸ B. A. Barnett,¹⁵
 M. Barone,⁹ E. Barzi,⁹ G. Bauer,¹⁸ T. Baumann,¹¹ F. Bedeschi,²⁶ S. Behrends,³ S. Belforte,²⁶
 G. Bellettini,²⁶ J. Bellinger,³⁷ D. Benjamin,³⁴ J. Benloch,¹⁸ J. Bensinger,³ D. Benton,²⁵
 A. Beretvas,⁷ J. P. Berge,⁷ J. Berryhill,⁵ S. Bertolucci,⁹ B. Bevensee,²⁵ A. Bhatti,³⁰
 K. Biery,⁷ M. Binkley,⁷ D. Bisello,²⁴ R. E. Blair,¹ C. Blocker,³ A. Bodek,²⁹ W. Bokhari,¹⁸
 V. Bolognesi,² G. Bolla,²⁸ D. Bortoletto,²⁸ J. Boudreau,²⁷ L. Breccia,² C. Bromberg,²⁰
 N. Bruner,²¹ E. Buckley-Geer,⁷ H. S. Budd,²⁹ K. Burkett,¹⁹ G. Busetto,²⁴ A. Byon-Wagner,⁷
 K. L. Byrum,¹ J. Cammerata,¹⁵ C. Campagnari,⁷ M. Campbell,¹⁹ A. Caner,²⁶ W. Carithers,¹⁷
 D. Carlsmith,³⁷ A. Castro,²⁴ D. Cauz,²⁶ Y. Cen,²⁹ F. Cervelli,²⁶ P. S. Chang,³² P. T. Chang,³²
 H. Y. Chao,³² J. Chapman,¹⁹ M. -T. Cheng,³² G. Chiarelli,²⁶ T. Chikamatsu,³⁵ C. N. Chiou,³²
 L. Christofek,¹³ S. Cihangir,⁷ A. G. Clark,¹⁰ M. Cobal,²⁶ E. Cocca,²⁶ M. Contreras,⁵
 J. Conway,³¹ J. Cooper,⁷ M. Cordelli,⁹ C. Couyoumtzelis,¹⁰ D. Crane,¹ D. Cronin-Hennessy,⁶
 R. Culbertson,⁵ T. Daniels,¹⁸ F. DeJongh,⁷ S. Delchamps,⁷ S. Dell'Agnello,²⁶ M. Dell'Orso,²⁶
 R. Demina,⁷ L. Demortier,³⁰ M. Deninno,² P. F. Derwent,⁷ T. Devlin,³¹ J. R. Dittmann,⁶
 S. Donati,²⁶ J. Done,³³ T. Dorigo,²⁴ A. Dunn,¹⁹ N. Eddy,¹⁹ K. Einsweiler,¹⁷ J. E. Elias,⁷
 R. Ely,¹⁷ E. Engels, Jr.,²⁷ D. Errede,¹³ S. Errede,¹³ Q. Fan,²⁹ G. Feild,³⁸ C. Ferretti,²⁶ I. Fiori,²
 B. Flaughner,⁷ G. W. Foster,⁷ M. Franklin,¹¹ M. Frautschi,³⁴ J. Freeman,⁷ J. Friedman,¹⁸
 Y. Fukui,¹⁶ S. Funaki,³⁵ S. Galeotti,²⁶ M. Gallinaro,²⁵ O. Ganel,³⁴ M. Garcia-Sciveres,¹⁷
 A. F. Garfinkel,²⁸ C. Gay,¹¹ S. Geer,⁷ D. W. Gerdes,¹⁵ P. Giannetti,²⁶ N. Giokaris,³⁰
 P. Giromini,⁹ G. Giusti,²⁶ L. Gladney,²⁵ D. Glenzinski,¹⁵ M. Gold,²¹ J. Gonzalez,²⁵

A. Gordon,¹¹ A. T. Goshaw,⁶ Y. Gotra,²⁴ K. Goulianos,³⁰ H. Grassmann,²⁶ L. Groer,³¹
 C. Grosso-Pilcher,⁵ G. Guillian,¹⁹ R. S. Guo,³² C. Haber,¹⁷ E. Hafen,¹⁸ S. R. Hahn,⁷
 R. Hamilton,¹¹ R. Handler,³⁷ R. M. Hans,³⁸ F. Happacher,⁹ K. Hara,³⁵ A. D. Hardman,²⁸
 B. Harral,²⁵ R. M. Harris,⁷ S. A. Hauger,⁶ J. Hauser,⁴ C. Hawk,³¹ E. Hayashi,³⁵ J. Heinrich,²⁵
 B. Hinrichsen,¹⁴ K. D. Hoffman,²⁸ M. Hohlmann,⁵ C. Holck,²⁵ R. Hollebeek,²⁵ L. Holloway,¹³
 A. Hölscher,¹⁴ S. Hong,¹⁹ G. Houk,²⁵ P. Hu,²⁷ B. T. Huffman,²⁷ R. Hughes,²² J. Huston,²⁰
 J. Huth,¹¹ J. Hylen,⁷ H. Ikeda,³⁵ M. Incagli,²⁶ J. Incandela,⁷ G. Introzzi,²⁶ J. Iwai,³⁵
 Y. Iwata,¹² H. Jensen,⁷ U. Joshi,⁷ R. W. Kadel,¹⁷ E. Kajfasz,²⁴ H. Kambara,¹⁰ T. Kamon,³³
 T. Kaneko,³⁵ K. Karr,³⁶ H. Kasha,³⁸ Y. Kato,²³ T. A. Keaffaber,²⁸ L. Keeble,⁹ K. Kelley,¹⁸
 R. D. Kennedy,⁷ R. Kephart,⁷ P. Kesten,¹⁷ D. Kestenbaum,¹¹ R. M. Keup,¹³ H. Keutelian,⁷
 F. Keyvan,⁴ B. Kharadia,¹³ B. J. Kim,²⁹ D. H. Kim,^{7a} H. S. Kim,¹⁴ S. B. Kim,¹⁹
 S. H. Kim,³⁵ Y. K. Kim,¹⁷ L. Kirsch,³ P. Koehn,²⁹ K. Kondo,³⁵ J. Konigsberg,⁸ S. Kopp,⁵
 K. Kordas,¹⁴ A. Korytov,⁸ W. Koska,⁷ E. Kovacs,^{7a} W. Kowald,⁶ M. Krasberg,¹⁹ J. Kroll,⁷
 M. Kruse,²⁹ T. Kuwabara,³⁵ S. E. Kuhlmann,¹ E. Kuns,³¹ A. T. Laasanen,²⁸ S. Lami,²⁶
 S. Lammel,⁷ J. I. Lamoureux,³ T. LeCompte,¹ S. Leone,²⁶ J. D. Lewis,⁷ P. Limon,⁷
 M. Lindgren,⁴ T. M. Liss,¹³ Y. C. Liu,³² N. Lockyer,²⁵ O. Long,²⁵ C. Loomis,³¹ M. Loretì,²⁴
 J. Lu,³³ D. Lucchesi,²⁶ P. Lukens,⁷ S. Lusin,³⁷ J. Lys,¹⁷ K. Maeshima,⁷ A. Maghakian,³⁰
 P. Maksimovic,¹⁸ M. Mangano,²⁶ J. Mansour,²⁰ M. Mariotti,²⁴ J. P. Marriner,⁷ A. Martin,³⁸
 J. A. J. Matthews,²¹ R. Mattingly,¹⁸ P. McIntyre,³³ P. Melese,³⁰ A. Menzione,²⁶ E. Meschi,²⁶
 S. Metzler,²⁵ C. Miao,¹⁹ T. Miao,⁷ G. Michail,¹¹ R. Miller,²⁰ H. Minato,³⁵ S. Miscetti,⁹
 M. Mishina,¹⁶ H. Mitsushio,³⁵ T. Miyamoto,³⁵ S. Miyashita,³⁵ N. Moggi,²⁶ Y. Morita,¹⁶
 J. Mueller,²⁷ A. Mukherjee,⁷ T. Muller,⁴ P. Murat,²⁶ H. Nakada,³⁵ I. Nakano,³⁵ C. Nelson,⁷
 D. Neuberger,⁴ C. Newman-Holmes,⁷ C-Y. P. Ngan,¹⁸ M. Ninomiya,³⁵ L. Nodulman,¹
 S. H. Oh,⁶ K. E. Ohl,³⁸ T. Ohmoto,¹² T. Ohsugi,¹² R. Oishi,³⁵ M. Okabe,³⁵ T. Okusawa,²³
 R. Oliveira,²⁵ J. Olsen,³⁷ C. Pagliarone,² R. Paoletti,²⁶ V. Papadimitriou,³⁴ S. P. Pappas,³⁸
 N. Parashar,²⁶ S. Park,⁷ A. Parri,⁹ J. Patrick,⁷ G. Pauletta,²⁶ M. Paulini,¹⁷ A. Perazzo,²⁶
 L. Pescara,²⁴ M. D. Peters,¹⁷ T. J. Phillips,⁶ G. Piacentino,² M. Pillai,²⁹ K. T. Pitts,⁷
 R. Plunkett,⁷ L. Pondrom,³⁷ J. Proudfoot,¹ F. Ptohos,¹¹ G. Punzi,²⁶ K. Ragan,¹⁴ D. Reher,¹⁷

A. Ribon,²⁴ F. Rimondi,² L. Ristori,²⁶ W. J. Robertson,⁶ T. Rodrigo,²⁶ S. Rolli,³⁶
 J. Romano,⁵ L. Rosenson,¹⁸ R. Roser,¹³ T. Saab,¹⁴ W. K. Sakumoto,²⁹ D. Saltzberg,⁵
 A. Sansoni,⁹ L. Santi,²⁶ H. Sato,³⁵ P. Schlabach,⁷ E. E. Schmidt,⁷ M. P. Schmidt,³⁸
 A. Scribano,²⁶ S. Segler,⁷ S. Seidel,²¹ Y. Seiya,³⁵ G. Sganos,¹⁴ M. D. Shapiro,¹⁷ N. M. Shaw,²⁸
 Q. Shen,²⁸ P. F. Shepard,²⁷ M. Shimojima,³⁵ M. Shochet,⁵ J. Siegrist,¹⁷ A. Sill,³⁴
 P. Sinervo,¹⁴ P. Singh,²⁷ J. Skarha,¹⁵ K. Sliwa,³⁶ F. D. Snider,¹⁵ T. Song,¹⁹ J. Spalding,⁷
 T. Speer,¹⁰ P. Sphicas,¹⁸ F. Spinella,²⁶ M. Spiropulu,¹¹ L. Spiegel,⁷ L. Stanco,²⁴ J. Steele,³⁷
 A. Stefanini,²⁶ K. Strahl,¹⁴ J. Strait,⁷ R. Ströhmer,^{7a} D. Stuart,⁷ G. Sullivan,⁵ K. Sumorok,¹⁸
 J. Suzuki,³⁵ T. Takada,³⁵ T. Takahashi,²³ T. Takano,³⁵ K. Takikawa,³⁵ N. Tamura,¹²
 B. Tannenbaum,²¹ F. Tartarelli,²⁶ W. Taylor,¹⁴ P. K. Teng,³² Y. Teramoto,²³ S. Tether,¹⁸
 D. Theriot,⁷ T. L. Thomas,²¹ R. Thun,¹⁹ M. Timko,³⁶ P. Tipton,²⁹ A. Titov,³⁰ S. Tkaczyk,⁷
 D. Toback,⁵ K. Tollefson,²⁹ A. Tollestrup,⁷ W. Trischuk,¹⁴ J. F. de Troconiz,¹¹ S. Truitt,¹⁹
 J. Tseng,¹⁸ N. Turini,²⁶ T. Uchida,³⁵ N. Uemura,³⁵ F. Ukegawa,²⁵ G. Unal,²⁵ J. Valls,^{7a}
 S. C. van den Brink,²⁷ S. Vejcik, III,¹⁹ G. Velez,²⁶ R. Vidal,⁷ R. Vilar,^{7a} M. Vondracek,¹³
 D. Vucinic,¹⁸ R. G. Wagner,¹ R. L. Wagner,⁷ J. Wahl,⁵ N. B. Wallace,²⁶ A. M. Walsh,³¹
 C. Wang,⁶ C. H. Wang,³² J. Wang,⁵ M. J. Wang,³² Q. F. Wang,³⁰ A. Warburton,¹⁴
 T. Watts,³¹ R. Webb,³³ C. Wei,⁶ C. Wendt,³⁷ H. Wenzel,¹⁷ W. C. Wester, III,⁷
 A. B. Wicklund,¹ E. Wicklund,⁷ R. Wilkinson,²⁵ H. H. Williams,²⁵ P. Wilson,⁵ B. L. Winer,²²
 D. Winn,¹⁹ D. Wolinski,¹⁹ J. Wolinski,²⁰ S. Worm,²¹ X. Wu,¹⁰ J. Wyss,²⁴ A. Yagil,⁷ W. Yao,¹⁷
 K. Yasuoka,³⁵ Y. Ye,¹⁴ G. P. Yeh,⁷ P. Yeh,³² M. Yin,⁶ J. Yoh,⁷ C. Yosef,²⁰ T. Yoshida,²³
 D. Yovanovitch,⁷ I. Yu,⁷ L. Yu,²¹ J. C. Yun,⁷ A. Zanetti,²⁶ F. Zetti,²⁶ L. Zhang,³⁷ W. Zhang,²⁵
 and S. Zucchelli²

(CDF Collaboration)

¹ *Argonne National Laboratory, Argonne, Illinois 60439*

² *Istituto Nazionale di Fisica Nucleare, University of Bologna, I-40127 Bologna, Italy*

³ *Brandeis University, Waltham, Massachusetts 02264*

- ⁴ *University of California at Los Angeles, Los Angeles, California 90024*
- ⁵ *University of Chicago, Chicago, Illinois 60638*
- ⁶ *Duke University, Durham, North Carolina 28708*
- ⁷ *Fermi National Accelerator Laboratory, Batavia, Illinois 60510*
- ⁸ *University of Florida, Gainesville, FL 33611*
- ⁹ *Laboratori Nazionali di Frascati, Istituto Nazionale di Fisica Nucleare, I-00044 Frascati, Italy*
- ¹⁰ *University of Geneva, CH-1211 Geneva 4, Switzerland*
- ¹¹ *Harvard University, Cambridge, Massachusetts 02138*
- ¹² *Hiroshima University, Higashi-Hiroshima 724, Japan*
- ¹³ *University of Illinois, Urbana, Illinois 61801*
- ¹⁴ *Institute of Particle Physics, McGill University, Montreal H3A 2T8, and University of Toronto,
Toronto M5S 1A7, Canada*
- ¹⁵ *The Johns Hopkins University, Baltimore, Maryland 21218*
- ¹⁶ *National Laboratory for High Energy Physics (KEK), Tsukuba, Ibaraki 315, Japan*
- ¹⁷ *Ernest Orlando Lawrence Berkeley National Laboratory, Berkeley, California 94720*
- ¹⁸ *Massachusetts Institute of Technology, Cambridge, Massachusetts 02139*
- ¹⁹ *University of Michigan, Ann Arbor, Michigan 48109*
- ²⁰ *Michigan State University, East Lansing, Michigan 48824*
- ²¹ *University of New Mexico, Albuquerque, New Mexico 87132*
- ²² *The Ohio State University, Columbus, OH 4320*
- ²³ *Osaka City University, Osaka 588, Japan*
- ²⁴ *Universita di Padova, Istituto Nazionale di Fisica Nucleare, Sezione di Padova, I-36132 Padova, Italy*
- ²⁵ *University of Pennsylvania, Philadelphia, Pennsylvania 19104*
- ²⁶ *Istituto Nazionale di Fisica Nucleare, University and Scuola Normale Superiore of Pisa, I-56100 Pisa,
Italy*
- ²⁷ *University of Pittsburgh, Pittsburgh, Pennsylvania 15270*
- ²⁸ *Purdue University, West Lafayette, Indiana 47907*
- ²⁹ *University of Rochester, Rochester, New York 14628*

³⁰ *Rockefeller University, New York, New York 10021*

³¹ *Rutgers University, Piscataway, New Jersey 08854*

³² *Academia Sinica, Taipei, Taiwan 11530, Republic of China*

³³ *Texas A&M University, College Station, Texas 77843*

³⁴ *Texas Tech University, Lubbock, Texas 79409*

³⁵ *University of Tsukuba, Tsukuba, Ibaraki 315, Japan*

³⁶ *Tufts University, Medford, Massachusetts 02155*

³⁷ *University of Wisconsin, Madison, Wisconsin 53806*

³⁸ *Yale University, New Haven, Connecticut 06511*

We present a study of J/ψ and $\psi(2S)$ production in $p\bar{p}$ collisions, at $\sqrt{s} = 1.8$ TeV with the CDF detector at Fermilab. The J/ψ and $\psi(2S)$ mesons are reconstructed using their $\mu^+\mu^-$ decay modes. We have measured the inclusive production cross section for both mesons as a function of their transverse momentum in the central region, $|\eta| < 0.6$. We also measure the fraction of events originating from b hadrons. We thus extract individual cross sections for J/ψ and $\psi(2S)$ mesons from b -quark decays and prompt production. We find a large excess (approximately a factor 50) of direct $\psi(2S)$ production compared with predictions from the Color Singlet Model.

PACS numbers: 13.85.Ni, 14.40.Gx

In high energy $p\bar{p}$ collisions charmonium particles predominantly come from prompt QCD production and the decay of b hadrons [1]. In the Color Singlet Model (CSM) for charmonium [2] the dominant source of prompt J/ψ mesons is χ_c production. Other sources of prompt J/ψ and $\psi(2S)$ mesons are expected to be negligible. However, we have reported production cross sections for both J/ψ and $\psi(2S)$ mesons at $\sqrt{s} = 1.8$ TeV that are higher than expectations and have a different P_T spectrum [3]. Similarly, measurements of the J/ψ cross section by UA1 [4] at $\sqrt{s} = 0.63$ TeV and the D0 experiment [5] indicate that the measured transverse momentum (P_T) spectrum of J/ψ mesons is not in agreement with

predictions for χ_c and b hadron decays alone. In this paper, we use the silicon vertex detector (SVX) in CDF to separate prompt ψ 's ($\psi \equiv J/\psi, \psi(2S)$ in what follows) from ψ 's from b hadron decays. We extract the production cross sections for prompt ψ mesons and find them to be much larger than the CSM predictions.

The CDF detector has been described in detail elsewhere [6]. Muons are reconstructed by matching track segments found in the central muon system (CMU), which covers the region $|\eta| < 0.6$ [7], to charged particle tracks reconstructed in the central tracking chamber (CTC). Approximately 60% of the muon tracks also have hits in the silicon vertex detector which provides measurements in the r - ϕ plane only, resulting in a track impact parameter resolution of $(13 + 40/P_T) \mu\text{m}$ where P_T (in GeV/c) is the track momentum transverse to the beam line. The data sample consists of $17.8 \pm 0.6 \text{ pb}^{-1}$ of $p\bar{p}$ collisions at $\sqrt{s} = 1.8$ TeV from the 1992-93 data taking period, collected using dimuon triggers in the CDF three-level trigger system. The Level 1 dimuon trigger requires two track segments in the CMU, separated by at least 5° in azimuth. The trigger efficiency for each muon at Level 1 rises from 50% at $P_T = 1.6 \text{ GeV}/c$ to 90% at $P_T = 3.1 \text{ GeV}/c$ with a plateau of 94%. The Level 2 trigger requires that at least one of the muon track segments is matched in ϕ to a track found in the CTC by the CFT [8], a hardware track-finding processor. The efficiency for finding a track with the CFT rises from 50% at $P_T = 2.7 \text{ GeV}/c$ to 90% at $P_T = 3.1 \text{ GeV}/c$ and reaches a plateau of 93%. The Level 3 trigger requires a pair of oppositely-charged muons after full track reconstruction.

A period with reduced Level 3 tracking efficiency is excluded from the J/ψ analysis where the data sample is large, but is included in the $\psi(2S)$ analysis with a correction derived from the J/ψ sample. The considered integrated luminosity is 15.4 pb^{-1} and 17.8 pb^{-1} for the J/ψ and $\psi(2S)$ sample, respectively. When the fraction of ψ 's from b decays is measured, an additional $\sim 90 \text{ pb}^{-1}$ of data from the 1994-95 Collider Run is added to the sample. This data sample is not included in the cross section measurement because the trigger and reconstruction efficiencies are still under study.

Reconstructed muons are required to have CMU hits consistent with the CTC track.

The CTC track is extrapolated to the CMU chambers and is required to lie within 3σ of the CMU hits, where σ is the uncertainty in the extrapolated position due to multiple scattering. The calorimeter tower in front of the muon chamber segment is required to have non-zero energy deposition. To remain in the region of good trigger efficiency, both muons are required to have $P_T > 2.0$ GeV/ c , and one muon is required to have $P_T > 2.8$ GeV/ c . The two muon tracks are fit with the requirement that they originate from a common point. We require that the one degree-of-freedom fit have $\chi^2 < 10$. Where available, we use SVX information to improve the track measurement. To remain in the region of good acceptance to ψ decays, the ψ candidate is required to satisfy $|\eta| < 0.6$ and $P_T > 5$ GeV/ c . The resulting mass distributions are shown in Fig. 1. There are approximately 22100 J/ψ and 800 $\psi(2S)$ candidates.

The number of ψ candidates in the data is determined by fitting the $\mu^+\mu^-$ invariant mass distribution with templates generated from Monte Carlo simulation of $\psi \rightarrow \mu^+\mu^-$ and $\psi \rightarrow \mu^+\mu^-\gamma$ decays. The muon momenta are smeared to simulate the detector resolution. Since the resulting $\mu^+\mu^-$ invariant mass resolution is a function of the transverse momentum of the ψ , the data are fit separately in each bin in $P_T(\psi)$. To correct for the trigger efficiency ($\epsilon_{\text{trigger}}$), which is a function of the muon P_T , each event is weighting by $1/\epsilon_{\text{trigger}}$, and the mass distribution is fit to the signal shape fixed from the simulation plus a linear background.

The ψ differential cross section is defined by

$$\frac{d\sigma(\psi)}{dP_T} \cdot \mathcal{B}(\psi \rightarrow \mu^+\mu^-) = \frac{N(\psi)}{\epsilon \cdot \int \mathcal{L} dt \cdot \Delta P_T}$$

where $N(\psi)$ is the number of ψ candidates in the bin corrected for the trigger efficiency, $\int \mathcal{L} dt$ is the integrated luminosity, ΔP_T is the size of the P_T bin and ϵ is the product of the detector and kinematic acceptance, the efficiencies of the event reconstruction and event selection requirements, whereas $\mathcal{B}(\psi \rightarrow \mu^+\mu^-)$ is the branching fraction for the decay $\psi \rightarrow \mu^+\mu^-$.

The acceptance is determined from Monte Carlo simulation. ψ events are generated with a flat distribution in P_T , η and ϕ . A parameterized detector simulation is used, and the

kinematic requirements are then applied to the generated events. The acceptance is found to rise from 9% at $P_T(\psi) = 5 \text{ GeV}/c$ to a plateau value of 28% for $P_T(\psi) > 14 \text{ GeV}/c$. The acceptance also depends on the ψ polarization. Taking θ^* to be the angle between the ψ direction in the lab frame and the μ^+ direction in the ψ rest frame, the angular distribution of the decay will have the form $1 + \alpha \cos^2 \theta^*$, where α ($-1 \leq \alpha \leq 1$) describes the polarization of the parent ψ . The magnitude of the uncertainty on the ψ acceptance will be different for prompt ψ 's and ψ 's from b hadron decays. Prompt ψ 's can in principle be fully polarized. From a Monte Carlo simulation of b hadron decays, we estimate that a ψ hadron with a polarization of $+1$ (-1) in the b hadron rest frame will have an effective polarization of only 0.143 (-0.219) in the ψ rest frame. We assign half of the maximum change in the acceptance (corresponding to changing α between -1 and $+1$) in each P_T bin as the uncertainty in each case. This uncertainty varies with $P_T(\psi)$, from 15% at $P_T(\psi) = 5 \text{ GeV}/c$ to 5% at $P_T(\psi) = 20 \text{ GeV}/c$.

The efficiency of the CMU segment reconstruction is measured using dimuon events recorded with a single muon trigger to be $97.2 \pm 1.2\%$. The efficiency of the CTC track reconstruction is measured by embedding hits from Monte Carlo-simulated particle tracks in data events, and attempting to reconstruct the added track. This efficiency is found to depend on the number of tracks near the embedded track. Only approximately 3% percent of the data have tracks where the efficiency to find the track is less than its plateau value of 98.4%. The average efficiency for reconstructing both CTC tracks is $96.4 \pm 2.8\%$. The efficiency of the CMU-CTC matching requirements is estimated from the number of J/ψ events before and after the matching requirements. The requirements are $90.5 \pm 1.0\%$ efficient.

Systematic uncertainties on the trigger efficiency are estimated by varying the functional form of the trigger efficiency, which is determined from dimuon events recorded with a single-muon trigger. Variation of the Level 1 trigger efficiency parameterization causes an uncertainty of 6.4%(6.1%) in the integrated J/ψ ($\psi(2S)$) cross sections. Similarly, there is a 1.1% (1.0%) systematic uncertainty in the J/ψ ($\psi(2S)$) cross section from the Level

2 trigger efficiency. Finally, the Level 3 trigger efficiency was estimated by examining the number of reconstructed muons found by the online requirements. These requirements are less efficient in the runs excluded from the J/ψ analysis, resulting in different efficiencies for the two states. The J/ψ efficiency is $97.0 \pm 0.2\%$, and the $\psi(2S)$ efficiency is $92.3 \pm 0.2\%$.

The integrated cross sections are

$$\begin{aligned}\sigma(J/\psi) \cdot \mathcal{B}(J/\psi \rightarrow \mu^+ \mu^-) &= 17.4 \pm 0.1 \text{ (stat)}_{-2.8}^{+2.6} \text{ (sys) nb} \\ \sigma(\psi(2S)) \cdot \mathcal{B}(\psi(2S) \rightarrow \mu^+ \mu^-) &= 0.57 \pm 0.04 \text{ (stat)}_{-0.09}^{+0.08} \text{ (sys) nb}\end{aligned}$$

where $\sigma(\psi) \equiv \sigma(p\bar{p} \rightarrow \psi X, P_T(\psi) > 5 \text{ GeV}/c, |\eta(\psi)| < 0.6)$.

We extract the fraction of ψ 's that originate from b hadrons using ψ candidates with both muons reconstructed in the SVX. The two muons are constrained to come from the same point which we refer to as the secondary vertex, to be distinguished from the primary vertex in the event. We measure the projection of the decay length onto the ψ transverse momentum, L_{xy} . This is converted into the proper lifetime of the assumed b hadron parent by $c\tau = L_{xy}/[(P_T(\psi)/m(\psi) \cdot F_{corr})]$, where $m(\psi)$ is the mass of the ψ state and F_{corr} is a correction factor, estimated from Monte Carlo simulations, that relates the boost factor $\beta\gamma$ of the ψ to the boost factor of the parent b hadron. Details of this procedure can be found in the measurement of the average b hadron lifetime [9].

The prompt component of the signal is parameterized by the resolution function, centered at $c\tau = 0$. The component of the signal due to b hadron decays is represented by an exponential of lifetime $c\tau_b$, convoluted with the resolution function. In this analysis we remove all track selection requirements described in [9] that may potentially affect the isolation of the ψ meson and thus the extracted fraction of ψ 's originating from b hadrons. As a result, the resolution function is augmented with two additional exponential tails. The tails constitute about 2% of the total number of candidates. We fix $c\tau_b$ to $438\mu\text{m}$, as found by the CDF inclusive b hadron lifetime measurement [9]. The lifetime and normalization of the remaining exponentials are left as free parameters in the fit.

The data $c\tau$ distribution is fit in each $P_T(\psi)$ bin using an unbinned log-likelihood fit.

The background fraction in the signal region is allowed to vary within the uncertainty in the normalization extracted from the ψ sidebands. The resulting fraction of ψ candidates originating from b hadron decays, $f_b(P_T)$, is shown as a function of $P_T(\psi)$ in Fig. 2. Several variations in the fitting technique produced an average relative variation of $\pm 0.9\%$, a value taken to be the systematic uncertainty on f_b due to the fitting procedure. Varying the average b hadron lifetime by one standard deviation changes f_b by $\pm 0.7\%$.

The cross section for ψ 's from b hadron decays is extracted by multiplying the fraction $f_b(P_T)$ with the inclusive ψ production cross section. The cross sections for ψ 's from b hadron decays are shown in Fig. 3. The theoretical predictions were calculated by generating b quarks according to the NLO QCD predictions [10], using a scale $\mu = \mu_0 \equiv \sqrt{m_b^2 + P_T^2}$ and $m_b = 4.75 \text{ GeV}/c^2$. The b quark is fragmented into b hadrons using Petersen fragmentation [11] with the fragmentation parameter, ϵ_b , set to 0.006. The b hadron is decayed to a ψX with a parameterization of the momentum distribution measured by the CLEO experiment [12]. Details of this procedure can be found in reference [13]. The data are higher than the QCD prediction by a factor 3-4 depending on $P_T(\psi)$. The uncertainty in the theoretical cross section (shown as the dashed and dotted curves in Fig. 3) is estimated by varying the scale μ to $\mu_0/4$ and $2\mu_0$ and ϵ_b to 0.004 and 0.008.

Multiplying the inclusive ψ cross section with the factor $(1 - f_B)$ results in the cross section for prompt ψ production, displayed in Fig. 4. Both cross sections are higher than theoretical predictions based on the Color Singlet Model [14] by a factor ~ 6 for J/ψ 's and a factor ~ 50 for $\psi(2S)$. In the case of $\psi(2S)$ mesons, where the transition $\chi_c \rightarrow \psi(2S)$ is kinematically forbidden, the interpretation of this prompt component is straightforward, as being due to direct $\psi(2S)$ production. In the case of J/ψ production, one must deconvolute various sources of prompt J/ψ mesons: the $\psi(2S) \rightarrow J/\psi$ transition, the $\chi_c \rightarrow J/\psi$ transition and direct J/ψ production. A measurement from the $\chi_c \rightarrow J/\psi\gamma$ transition is described in [15]. A recent model that attempts to explain this discrepancy with theoretical expectations is the Color Octet Model [16]. In this model, the shape of the cross section as a function of $P_T(\psi)$ is calculated perturbatively. However, the normalization depends on

non-perturbative matrix elements for which there exist only order of magnitude predictions. These amplitudes can in principle be measured by fitting the shapes calculated in [16] to the data.

In conclusion, we have measured the inclusive J/ψ and $\psi(2S)$ production cross sections. We have separated prompt ψ 's from ψ 's originating from b hadron decays. The b component is a factor of 3-4 higher than theoretical predictions. The prompt component is also higher than expectations from the Color Singlet Model. For $\psi(2S)$ mesons, the prompt data are more than an order of magnitude higher (approximately a factor 50) than the theoretical calculations. A possible explanation for this very large excess may come from the Color Octet Model introduced recently.

We thank the Fermilab staff and the technical staffs of the participating institutions for their vital contributions. This work was supported by the U.S. Department of Energy and National Science Foundation; the Italian Istituto Nazionale di Fisica Nucleare; the Ministry of Education, Science and Culture of Japan; the Natural Sciences and Engineering Research Council of Canada; the National Science Council of the Republic of China; and the A. P. Sloan Foundation.

-
- [1] E.W.N. Glover, A.D. Martin and W.J. Stirling, *Z. Phys.* **C38**, 473 (1988).
 - [2] R. Baier and R. Ruckl, *Z. Phys.* **C19**, 251 (1983).
 - [3] CDF Collaboration, F. Abe *et al.*, *Phys. Rev. Lett.* **69**, 3704 (1992).
 - [4] UA1 Collaboration, C. Albajar *et al.*, *Phys. Lett.* **B256**, 121 (1991).
 - [5] D0 Collaboration, S. Abachi *et al.*, *Phys. Lett.* **B370**, 239 (1996).
 - [6] F. Abe *et al.*, *Nucl. Instrum. Methods Phys. Res., Sect. A* **271**, 376 (1988), and references therein. The silicon vertex detector is described in F. Abe *et al.*, *Phys. Rev.* **D50**, 2966 (1994).
 - [7] In CDF, the positive z axis lies along the proton direction, r is the radius from this axis, θ is the polar angle and ϕ is the azimuthal angle. The pseudorapidity, η , is defined as $-\ln[\tan(\theta/2)]$.
 - [8] G. W. Foster *et al.*, *Nucl. Instrum. Methods Phys. Res., Sect. A* **269**, 93 (1988).
 - [9] CDF Collaboration, F. Abe *et al.*, *Phys. Rev. Lett.* **71**, 3421 (1993).
 - [10] P. Nason, S. Dawson and R.K. Ellis, *Nucl. Phys.* **B327**, 49 (1988).
 - [11] C. Petersen *et al.*, *Phys. Rev.* **D27**, 105 (1983).
 - [12] CLEO Collaboration, R. Balest *et al.*, Contributed Paper GLS0248 to the 27th International Conference on High-Energy Physics, Glasgow, Scotland, 1996.
 - [13] T. Daniels, Ph.D. dissertation, Massachusetts Institute of Technology, 1997.
 - [14] E. Braaten, M.A. Doncheski, S. Fleming and M.L. Mangano, *Phys. Lett.* **B333** 548 (1994);
M. Cacciari and M. Greco, *Phys. Rev. Lett.* **73**, 1586 (1994).
 - [15] CDF Collaboration, F. Abe *et al.*, “Production of J/ψ from χ_c decays in $p\bar{p}$ Collisions at $\sqrt{s} = 1.8$ TeV”, Fermilab Preprint FERMILAB-PUB-97/026-E, submitted to *Phys. Rev. Letters*.

- [16] E. Braaten and S. Fleming, Phys. Rev. Lett. **74**, 3327 (1995);
P. Cho and M. Wise, Phys. Lett. **B346**, 129 (1995);
M. Cacciari, M. Greco, M.L. Mangano and A. Petrelli, Phys. Lett. **B356**, 553 (1995);
P. Cho and A.K. Leibovich, Phys. Rev. **D53**, 150 (1996);
P. Cho and A.K. Leibovich, Phys. Rev. **D53**, 6203 (1996).

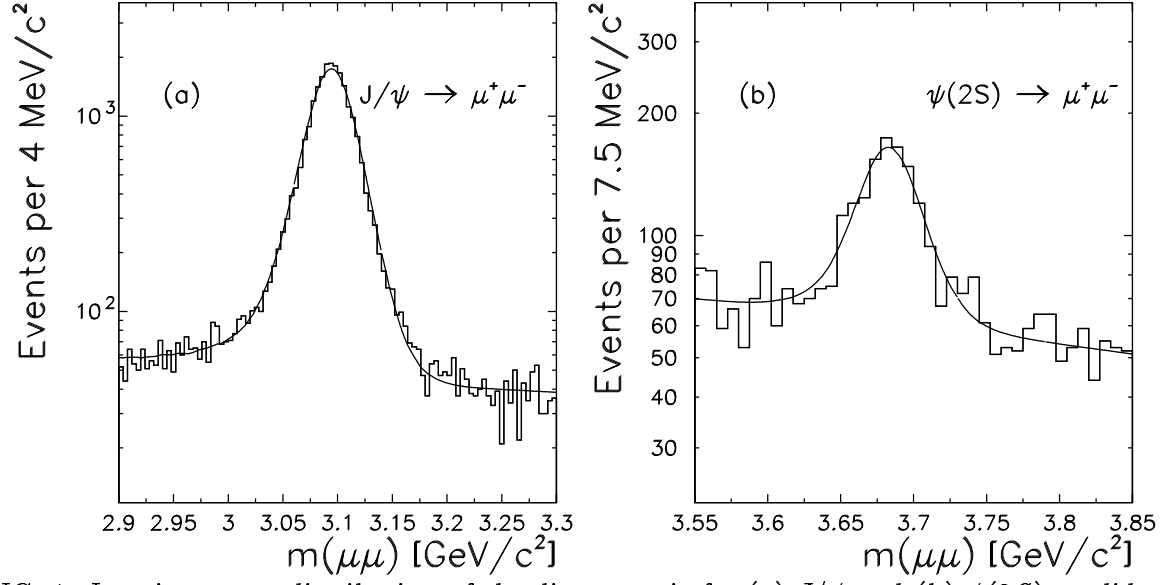


FIG. 1. Invariant mass distribution of the dimuon pair for (a) J/ψ and (b) $\psi(2S)$ candidates, after all selection requirements.

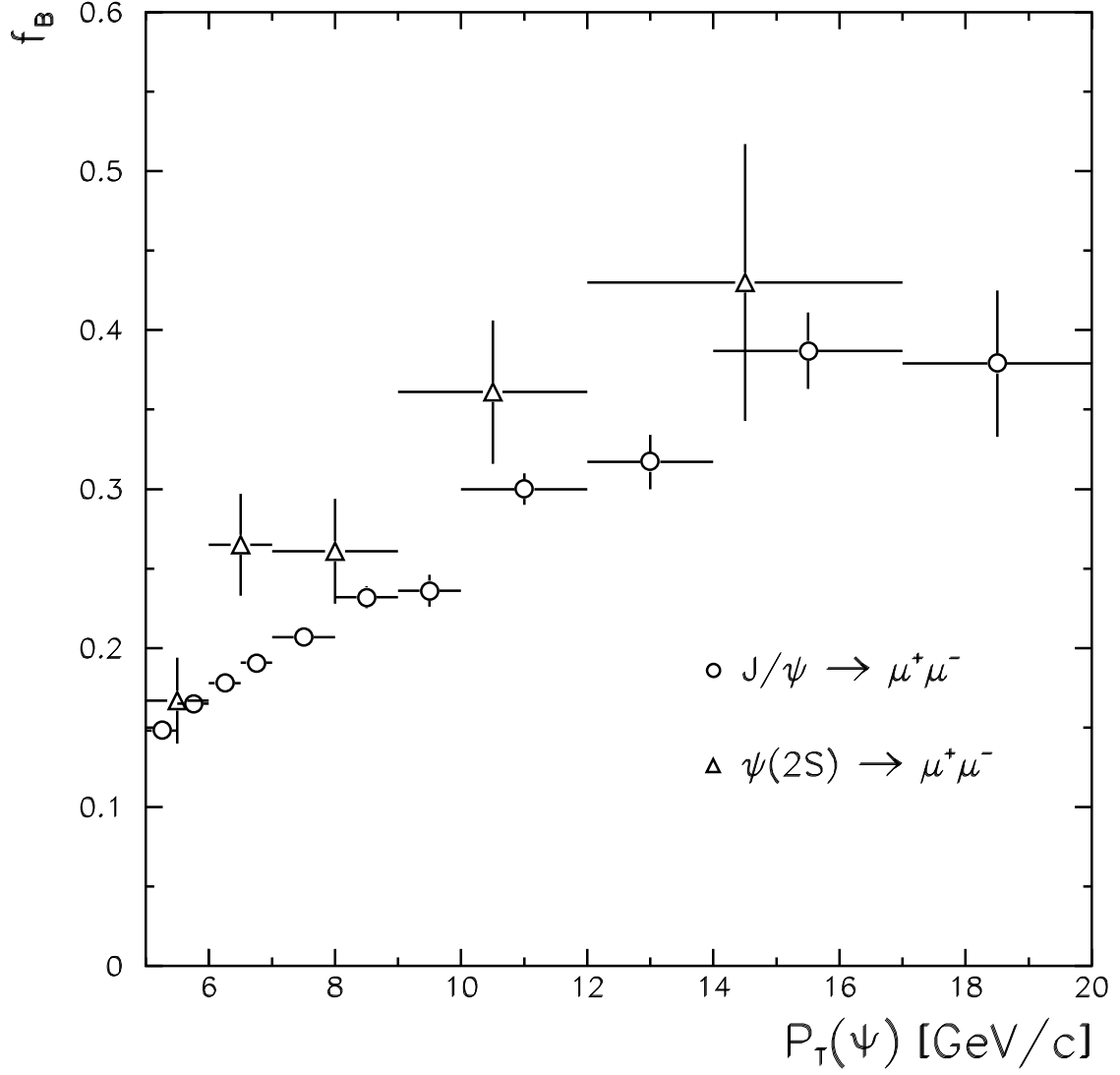


FIG. 2. The fractions of J/ψ (circles) and $\psi(2S)$ (triangles) originating from b -hadron decays. The error bars indicate the combined statistical and systematic uncertainties on the fractions.

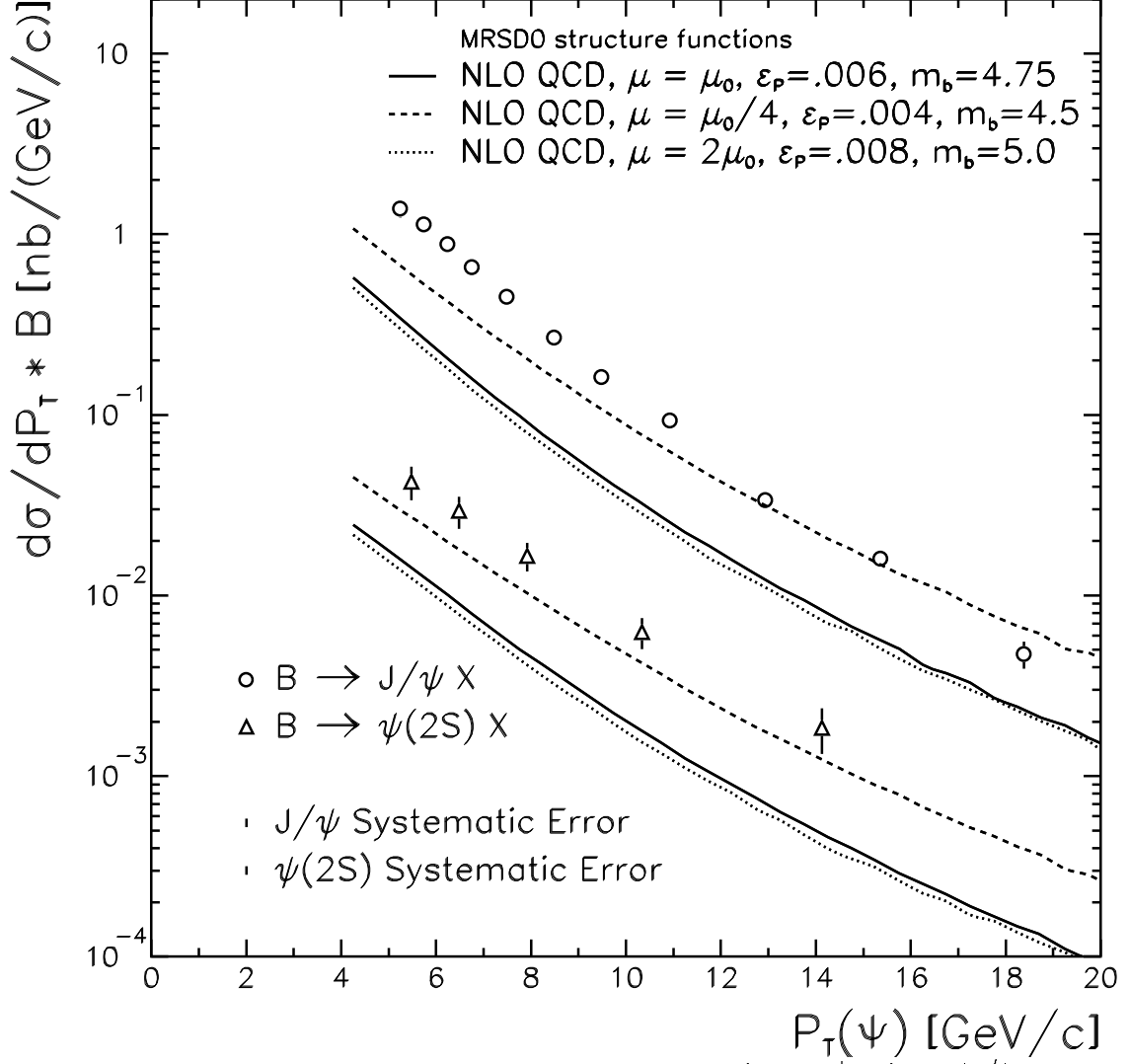


FIG. 3. The differential cross section times branching ratio, $\mathcal{B}(\psi \rightarrow \mu^+ \mu^-)$, for $|\eta^\psi| < 0.6$ for ψ mesons originating from b hadron decays. The solid lines indicate the theoretical predictions based on perturbative QCD. The dashed lines are based on the same calculation with the QCD scale, the mass of the b quark and the Petersen fragmentation parameter varied within their uncertainties.

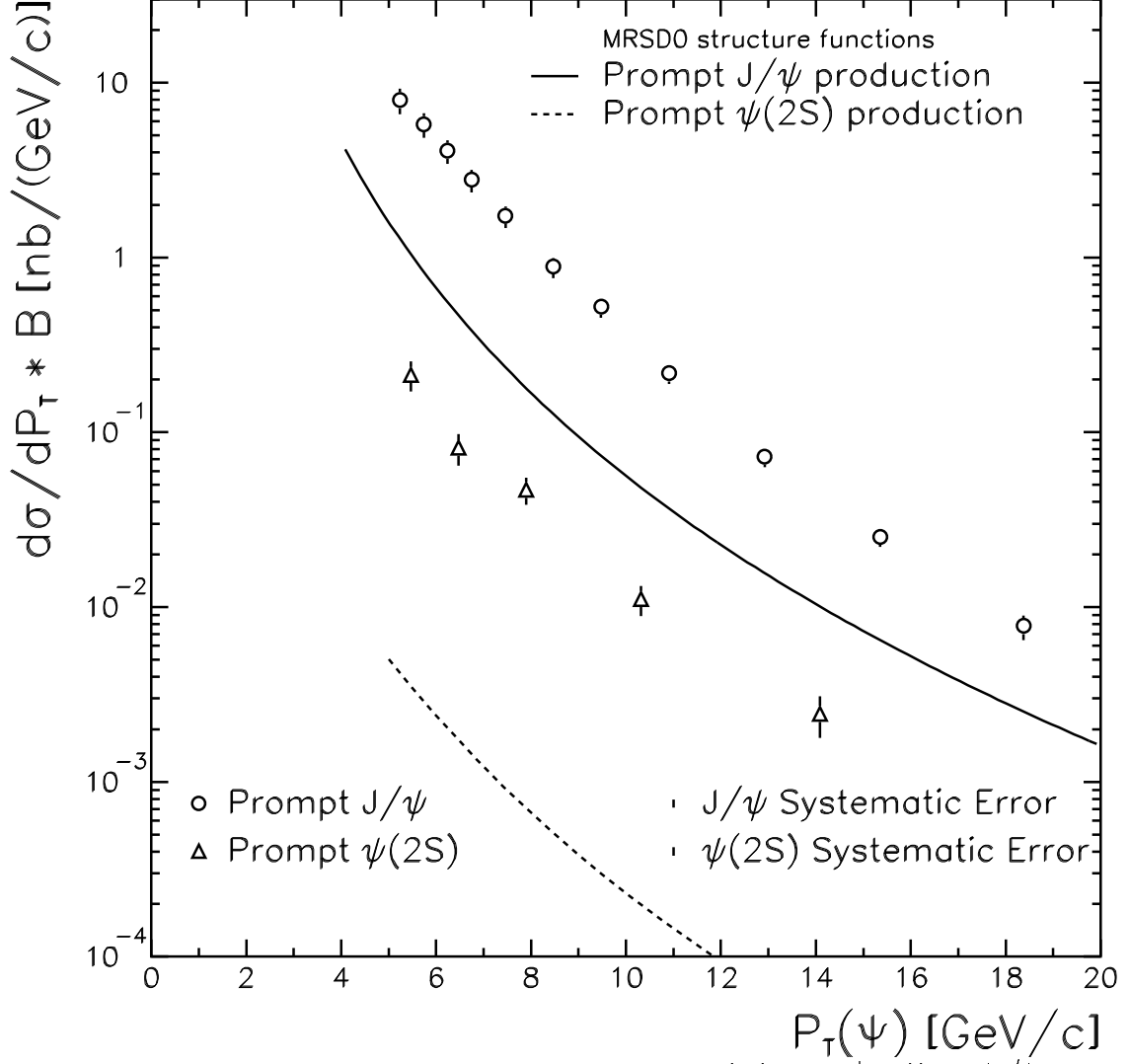


FIG. 4. The differential cross section times branching ratio ($\mathcal{B}(\psi \rightarrow \mu^+ \mu^-)$) for $|\eta^\psi| < 0.6$ for prompt ψ mesons. The vertical error bars are the statistical and the P_T -dependent systematic uncertainties, added in quadrature. Circles: J/ψ ; Triangles: $\psi(2S)$. The lines are the theoretical expectations based on the Color Singlet Model.